Effect of geometry and anisotropy of a Hele-Shaw cell on viscous fingering of polymer solutions

Masami Kawaguchi,* Atushi Shibata, Koukichi Shimomoto, and Tadaya Kato
Department of Chemistry for Materials, Faculty of Engineering, Mie University, 1515 Kamihama, Tsu, Mie 514-8507, Japan
(Received 6 February 1998)

Viscous fingering patterns of hydroxypropyl methyl cellulose (HPMC) solutions were investigated by forcing air in radial and linear geometry Hele-Shaw cells with radial and linear geometry as functions of HPMC concentration and applied pressure. The resulting patterns depended on the HPMC concentration and the cell geometry and anisotropy. The characteristic quantities of pattern growth, such as the finger tip velocity and the finger width, were evaluated. The tip velocity in the anisotropic linear cell was almost the same as that in the radial one, moreover, the finger width was well correlated with the pattern morphological changes. [S1063-651X(98)07807-6]

PACS number(s): 47.20.Gv, 47.54.+r, 61.25.Hq

INTRODUCTION

Viscous fingering patterns in the Hele-Shaw cell have been given a lot of attention in the past few decades, both experimentally and theoretically [1–19]. Our understanding of viscous fingering problems in non-Newtonian fluids such as polymer solutions is far less complete than those in simple Newtonian fluids. Recently, experiments using polymer solutions have been investigated by several research groups [3,12–19]. Zhao and Maher [13] studied the fingering experiments for aqueous solutions of polyethylene oxide (PEO) and hydrophobic end-capped PEO displaced by water in a radial Hele-Shaw cell. For the end-capped PEO solution a transition from tip splitting to fracturing was obtained by increasing the injection rate of water due to the strong chain entanglements, but the fingering-fracture transition was not observed for the PEO [14].

Very recently, Kawaguchi, Makino, and Kato [19] reported a morphological change from dense-branching to a skewering pattern through the tip-splitting pattern of aqueous high molecular weight hydroxypropyl methyl cellulose (HPMC) solutions in a radial Hele-Shaw cell pushed by air with an increase in injection pressure. From the results described above, it can be concluded that changes in the viscoelasticity of the more viscous liquid strongly influences the morphological transition of the fingering patterns. On the other hand, Bonn, Kellay, Ben Amar, and Meunier [16,17] investigated the viscous fingerings of aqueous solutions of PEO in a linear Hele-Shaw cell by injection of air. The measured finger widths largely deviated from those in the Newtonian fluids since finger tip velocity depends on dynamic interfacial tension and viscosity.

The effects of the geometry and anisotropy of the cell on the viscous fingering patterns in polymer solutions, however, have not been well investigated in comparison with the fingering experiments involving simple liquids, such as oils and aqueous glycerin solutions [1,2,5,7,20–25]. In this paper, we report the results of viscous fingering experiments using aqueous HPMC solutions in a radial Hele-Shaw cell, a linear one, and a linear one with anisotropy as functions of HPMC concentration and the injection pressure of air. The finger tip velocity will be compared with Darcy's law. Furthermore, morphological changes in the fingering patterns will also be discussed by taking into account the tip velocity and finger width.

EXPERIMENTAL SECTION

One HPMC with the molecular weight of 371×10^3 was dissolved in water at 0.1, 0.5, and 1.0 g/100 ml. In order to obtain high-contrast patterns, the HPMC solutions were colored by adding methylene blue. The fingering experiments were performed at 25 °C using three different Hele-Shaw cells: a radial cell made by using two plane-glass plates ($0.8\times50\times35$ cm^3) with a silicon wafer spacer of 0.05 cm thickness clamped in between the plates; isotropic and anisotropic linear cells made of the same two glass plates as the radial cell, clamped along their sides with a *U*-shaped silicon rubber sheet ($0.05\times50\times15$ cm^3) and with silicon wafer spacers of 0.05 cm thickness in between. In the linear cells, the width of the channel fixed at 5.0 cm by using the rubber sheet. For an anisotropic linear cell the upper plate was a glass plate with a thin groove with a triangular section of about 0.003 cm width and 0.001 cm depth from an inlet (0.2 cm in diameter) toward the unsealed edge.

The sample was injected through the inlet at the center of the top plate for the radial cell to form a 10-cm sample radius, whereas for the linear cells it was injected into the inlet at the distance of 10 cm from the short sealed edge of the top plate. Air was injected through the inlet under different injection pressures from 0.5 to 9.0 kPa, using the same pressure reservoir as described previously [18,19]. The generated patterns were recorded with a charge-coupled device video camera-recorder method. The images of the recorded patterns were printed by an image printer, and they were analyzed by a Himawari-60 digital image analyzer (Library Co. Tokyo). We can calculate an initial finger tip velocity V_i defined by fitting an initial straight line on the plot of a given distance from the inlet to the tip of the grown finger against the necessary time. More than 60 data points were used.

Rheological measurements of the HPMC solutions were performed using a Rheometrics ARES viscoelastic measurement system with a Couette geometry (outer cylinder diam-

*Author to whom correspondence should be addressed.

eter: 6.8 cm; inner cylinder diameter: 6.4 cm; immersion length: 3.34 cm in the shear rate range from 0.1 to 1262 s^{-1}. From the plots of the steady-state shear viscosity as a function of the shear rate for the HPMC solutions, the HPMC solutions of 1.0 and 0.5 g/100 ml displayed shear-thinning behavior clearly at shear rates higher than round 20 and 160 s^{-1}, respectively, and their concentrations are beyond an overlapping concentration of HPMC solution, 0.19 g/100 ml. The respective zero-shear rate shear viscosities, η_0 for 1.0 and 0.5 g/100 ml are 0.360 and 0.036 Pa s. On the other hand, the 0.1 g/100 ml HPMC solution behaved as a Newtonian fluid in the entire range of the shear rates studied and the shear viscosity was 0.0022 Pa s.

RESULTS AND DISCUSSION

Figure 1 (I) shows fingering patterns at 4.5 kPa in the radial cell. The fingering pattern of the 0.5 g/100 ml HPMC solution is a tip-splitting one, whereas the pattern of the 1.0 g/100 ml HPMC solution is different from the tip-splitting one and it is classified as a highly branched pattern. When the injection pressure increases, the finger width becomes thinner.

Figure 1 (II) shows finger patterns at 4.5 kPa in the isotropic linear cell. A single finger at the lowest concentration of the HPMC solution is similar to the Saffman-Taylor one [26]; however, at the injection pressures of 1.5 and 2.0 kPa narrow pointed fingers are observed. Similar results were observed for the PEO solutions at a lower tip velocity by Bonn, Kellay, Ben Amar, and Meunier [16,17]. The PEO solutions should not show clear shear thinning due to a lower concentration than the overlapping concentration.

For the 0.5 g/100 ml HPMC solution at the injection pressure of 4.5 kPa, a branching pattern is first developed and a tip-splitting pattern is later observed, namely a morphological transition in the fingering pattern. Such a pattern change usually occurs at the pressure gradient of around 150 Pa/cm, which can be calculated by the ratio of the applied injection pressure to the distance between the finger tip and the unsealed edge, irrespective of the injection pressure. Beyond the injection pressure of 6.0 kPa, the tip-splitting patterns are similar to those displayed in Fig. 1 (Ia) and the form of the resulting finger becomes less rounded with an increase in the injection pressure. Below the injection pressure of 4.5 kPa, on the other hand, only the branching pattern is observed. The highest concentration of HPMC solution shows only the branching pattern, and the skeletons become simple due to the pruning branches and the narrowing branches. The reason why either branched or tip-splitting fingers were observed at the higher HPMC concentration solutions should be attributed to the shear-thinning behavior.

Figure 1 (III) shows finger patterns at 4.5 kPa in the anisotropic linear cell. The lowest concentration of the HPMC solution shows narrower and more pointed fingering patterns than those observed in the isotropic cell. Furthermore, the shapes of more pointed fingering patterns are similar to those for Newtonian fluids in a grooved linear Hele-Shaw cell [22]. The width of the pointed finger decreases with an increase in the injection pressure. For the 1.0 g/100 ml HPMC solution, a finger tends to grow faster along the groove accompanied by side branches and a dendrite pattern is observed at any injection pressure. When the injection pressure increases, the finger width becomes narrower and the finger tip grows larger. The 0.5 g/100 ml HPMC solution shows the dendrite pattern and the side branches appear more infrequently than the 1.0 g/100 ml, and above the injection pressure of 4.5 kPa the dendrite pattern is drastically changed

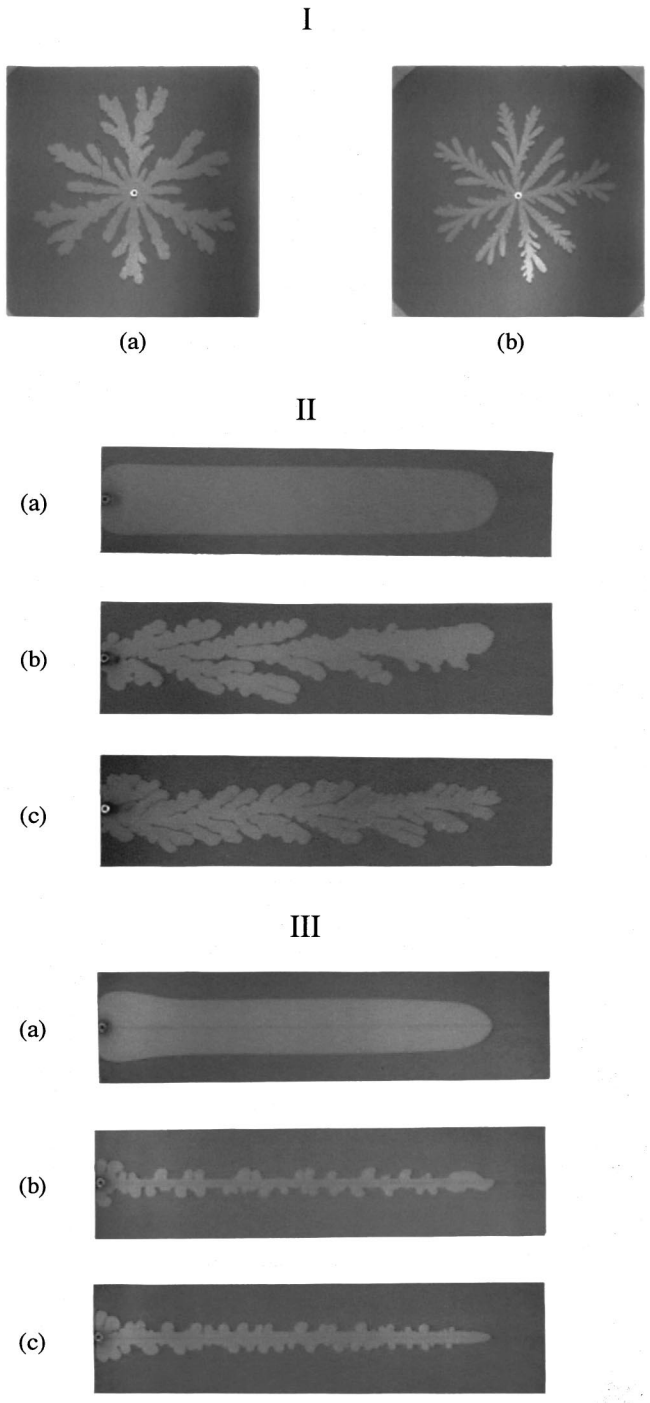

FIG. 1. Typical fingering patterns for the 0.5 (a) and 1.0 (b) g/100 ml HPMC solutions at 4.5 kPa in a radial cell (I), for the 0.1 (a), 0.5 (b), and 1.0 (c) g/100 ml HPMC solutions at 4.5 kPa in an isotropic linear cell (II), and for the 0.1 (a), 0.5 (b), and 1.0 (c) g/100 ml HPMC solutions at 4.5 kPa in an anisotropic linear cell (III). The diameter of the envelope of the patterns in the radial cell is 10 cm. The length of the growth of the patterns in the linear cells is 18 cm.

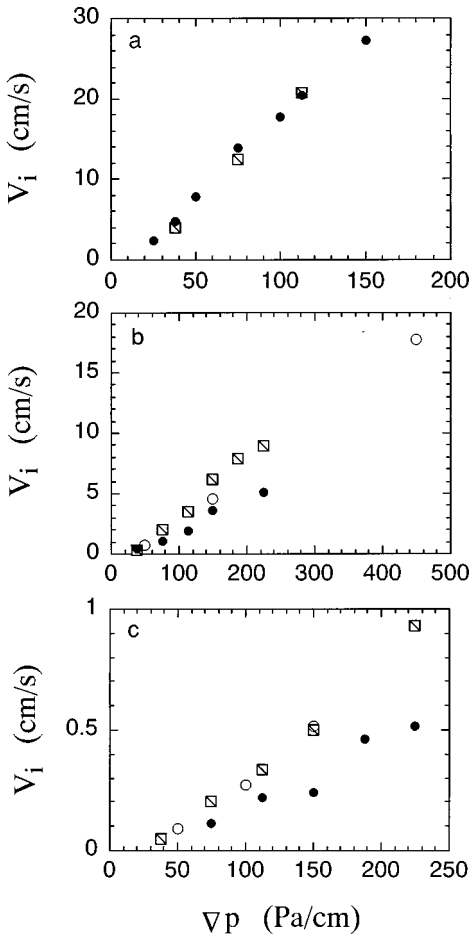

FIG. 2. Initial tip velocity V_i as a function of ∇p for the 0.1 (a), 0.5 (b), and 1.0 (c) g/100 ml HPMC solutions with different Hele-Shaw cells: radial cell (○), isotropic linear cell (●), and anisotropic linear cell (⊠).

into one which meanders along the groove. The pattern change is usually observed at the pressure gradient of around 200 Pa/cm, which is higher than that in the isotropic cell. The difference may be attributed to the fact that the flow instability occurs at larger velocities since the fingers in the anisotropic cell are more stable than those in the isotropic one.

In a Hele-Shaw cell experiment the velocity field in the high viscous fluid can be assumed to be two dimensional and proportional to pressure gradient ∇p as

$$v=(b^2/12\eta)\nabla p, \tag{1}$$

where v is the finger tip velocity, b is the plate separation of the Hele-Shaw cell, and η is the viscosity of the more viscous fluid. Equation (1) is well known as Darcy's law and it is satisfied in Newtonian fluids. The tip velocities for water and aqueous glycerin solution in our linear Hele-Shaw cells can be found to be in agreement with Darcy's law.

The plots of the initial tip velocity V_i against ∇p for the HPMC solutions, are shown in Fig. 2. At the lowest HPMC concentration V_i is independent of the anisotropy in the cell, but the velocity data appear to be fitted on a straight line without passing through the origin.

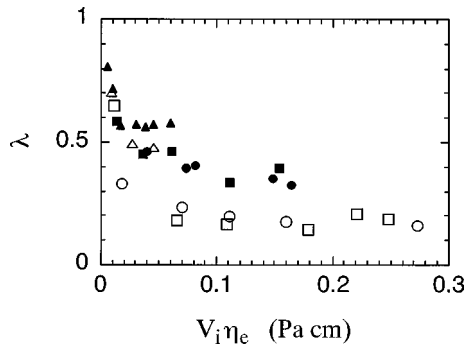

FIG. 3. The λ value as a function of the product of the initial tip velocity V_i and the effective viscosity η_e at the imposed shear rate for the 0.1 (triangles), 0.5 (squares), and 1.0 (circles) g/100 ml HPMC solutions in isotropic (filled symbols) and anisotropic (open symbols) cells.

For the higher concentration HPMC solutions, the values of V_i in the anisotropic linear cell are almost equal to those in the radial cell, are larger than those in the isotropic linear cell, and can be fitted on a straight line. The straight line fitting on the velocity data does not pass through the origin, and the interception point of the ∇p axis, approximately 30 Pa/cm, is almost independent of the HPMC concentration. Furthermore, below $\nabla p = 10$ Pa/cm the HPMC solutions cannot be replaced by air, namely the observation of the finger pattern growth. This shows the presence of a critical pressure gradient, beyond which the finger growth occurs. This growth seems to be attributed to some weak internal structures due to the interaction between the hydrophobic side chains. Such internal structures should be broken down by applied stress, leading to the shear-thinning behavior. Moreover, scattering the velocity data of the linear cells is mainly attributable to the morphological changes in the patterns. Thus, it can be concluded that the flow behavior of the HPMC solutions deviates from Darcy's law.

It is interesting to discuss the morphology transition at the 0.5 g/100 ml HPMC solution by taking into account its rheology. The imposed shear rates defined by the ratio of v to b [27] are calculated to be $160-170\ s^{-1}$ at $\nabla p = 200$ Pa/cm and they are in good agreement with the shear rate, above which the 0.5 g/100 ml HPMC solution shows shear thinning as mentioned above. The reason why no morphological transition is observed at the highest HPMC concentration, on the other hand, may be attributed to a gradual loosening of chain entanglements under shear flow because the higher the HPMC concentration, the stronger the chain entanglements.

The finger width is another important and characteristic parameter in understanding the fingering pattern, and it is well known to be related to the dimensionless parameter of $1/B = 12(\eta v/\gamma)(W/b)^2$ [28,29], where γ is the surface tension of fluid displaced and W is the channel width. Instead of the finger width, the relative ratio λ of the finger width to the value of W is usually employed. In the present experiment, we define the value of λ as the ratio of the area displaced by air over the total surface area until the distance from the inlet to a position in which the tip velocity is determined, irrespective of the fingering pattern. In Fig. 3, the values of λ for the HPMC solutions are plotted as a function of the product of V_i and an effective viscosity η_e at the imposed shear rates

defined by the ratio of v to b, instead of $1/B$, since the γ value=47.0 mN/m is constant independent of HPMC concentration. The η_e values are estimated from an interpolation of the plot of the steady-state shear viscosity as a function of the shear rate. The λ values in the isotropic cell are larger than those in the anisotropic one due to anisotropy and similar results were obtained in Newtonian fluids [20–22]. The value of λ in the isotropic cell for the 0.1 g/100 ml HPMC solution is larger than the Saffman-Taylor limiting value of 0.5 [26] and settles at a plateau value of 0.58. The wider deviation from the Saffman-Taylor limiting value was found in the experiments of dilute polymer solutions [16,17].

For the higher HPMC concentrations, the λ value tends to approach a plateau value in the respective cells, however, the λ value becomes somewhat wider when changes in the pattern morphology occur. The resulting plateau λ value in the isotropic cell is lower than the Saffman-Taylor limit due to shear-thinning behavior, and it is larger than that in the anisotropic cell. In conclusion, we have shown that the HPMC solutions in various Hele-Shaw cells exhibit systematic changes in the morphology of the fingering patterns as functions of the polymer concentration and the injection pressure. In particular, the resulting finger velocity in the radial cell is almost the same as that in the anisotropic linear cell and the pattern morphology changes can be well correlated with changes in the velocity as well as the finger width.

[1] E. Ben-Jacob, R. Godbey, N. D. Goldenfeld, J. Koplik, H. Levine, T. Mueller, and L. M. Sander, Phys. Rev. Lett. **55**, 1315 (1985).
[2] V. Horvath, T. Vicsek, and J. Kertesz, Phys. Rev. A **35**, 2353 (1987).
[3] G. Daccord, J. Nittmann, and H. E. Stanley, Phys. Rev. Lett. **56**, 336 (1986).
[4] A. Buka, J. Kertesz, and T. Vicsek, Nature (London) **323**, 424 (1986).
[5] Y. Couder, O. Cardoso, D. Dupuy, P. Tavernier, and W. Thom, Europhys. Lett. **2**, 437 (1986).
[6] S. Liang, Phys. Rev. A **33**, 2663 (1986).
[7] J.-D. Chen, Exp. Fluids **5**, 363 (1987).
[8] G. Zocchi, B. E. Shaw, A. Libchaber, and L. P. Kadanoff, Phys. Rev. A **36**, 1894 (1987).
[9] S. K. Sarkar and D. Jasnow, Phys. Rev. A **39**, 5299 (1989).
[10] E. Ben-Jacob and P. Garik, Nature (London) **343**, 523 (1990).
[11] E. Lemaire, P. Levitz, G. Daccord, and H. Van Damme, Phys. Rev. Lett. **67**, 2009 (1991).
[12] D. E. Smith, X. Z. Wu, A. Libchaber, E. Moses, and T. Witten, Phys. Rev. A **45**, R2165 (1992).
[13] H. Zhao and J. V. Maher, Phys. Rev. A **45**, R8328 (1992).
[14] H. Zhao and J. V. Maher, Phys. Rev. E **47**, 4278 (1993).
[15] S. S. Park and D. J. Durian, Phys. Rev. Lett. **72**, 3347 (1994).
[16] D. Bonn, H. Kellay, M. Ben Amar, and J. Meunier, Phys. Rev. Lett. **75**, 2132 (1995).
[17] D. Bonn, H. Kellay, M. Ben Amar, and J. Meunier, Physica A **220**, 60 (1995).
[18] K. Makino, M. Kawaguchi, K. Aoyama, and T. Kato, Phys. Fluids **7**, 455 (1995).
[19] M. Kawaguchi, K. Makino, and T. Kato, Fractals **4**, 181 (1996); Physica D **109**, 325 (1997).
[20] Y. Couder, N. Gerard, and M. Rabaud, Phys. Rev. A **34**, 5175 (1986).
[21] G. Zocchi, B. E. Shaw, A. Libchaber, and L. P. Kadanoff, Phys. Rev. A **36**, 1894 (1987).
[22] M. Rabaud, Y. Couder, and N. Gerard, Phys. Rev. A **37**, 935 (1988).
[23] H. Thome, M. Rabaud, V. Hakim, and Y. Couder, Phys. Fluids A **1**, 224 (1989).
[24] M. Ben Amar, R. Combescot, and Y. Couder, Phys. Rev. Lett. **70**, 3047 (1993).
[25] K. V. McCould and J. V. Maher, Phys. Rev. E **51**, 1184 (1995).
[26] P. G. Saffman and G. I. Taylor, Proc. R. Soc. London, Ser. A **245**, 312 (1958).
[27] H. Van Damme and E. Lamaie, in *Disorder and Fracture*, edited by J. C. Charnet, S. Roux, and E. Guyon (Plenum, New York, 1987), Chap. 6.1.
[28] D. Bensimon, L. P. Kadanoff, S. Liang, B. I. Shariman, and C. Tang, Rev. Mod. Phys. **58**, 977 (1986).
[29] P. Tabeling, G. Zocchi, and A. Libchaber, J. Fluid Mech. **177**, 67 (1987).